MAX-PLANCK-INSTITUT FÜR PLASMAPHYSIK

GARCHING BEI MÜNCHEN

Taking the Tokamak ß-limit into Account in a Simplified Rescaling of Existing Reactor Designs

A. F. Knobloch

IPP 4/220 March 1985

Die nachstehende Arbeit wurde im Rahmen des Vertrages zwischen dem Max-Planck-Institut für Plasmaphysik und der Europäischen Atomgemeinschaft über die Zusammenarbeit auf dem Gebiete der Plasmaphysik durchgeführt.

IPP 4/220

March 1985

Taking the tokamak ß-limit into account in a simplified rescaling of existing reactor designs.

A. F. Knobloch

Abstract

Since the IAEA conference of 1984 in London the existence of a quantitatively rather well defined ß-limit in tokamaks is no longer disputed. For the energy confinement time a scaling roughly proportional to the current seems to be indicated. In this report a number of consequences for a development step like INTOR and for a next possible step are pointed out, based on a simplified rescaling of existing conceptual designs with elongated plasma cross section. The approximate impact of a possible density limit is included in the discussion. Some quantitative conclusions on modifications to an INTOR like machine are drawn and the demanding requirements for a subsequent step are characterized.

Table of contents

1. Introduction

Since the IAEA conference of 1984 in London the existence of a quantitatively rather well defined β limit in tokamaks is no longer disputed. For the energy confinement time a scaling roughly proportional to the plasma current seems to be indicated.

Here a number of consequences for a development step like INTOR /1/ are pointed out and a look is taken at a next possible step.

Simplified scaling relations that show the essential effects of the β-limit are entirely sufficient for general considerations. The approximate impact of a possible density limit is also included in the discussion.

2. Relations for rescaling a tokamak reactor design

In view of the many detailed tokamak reactor designs available a rescaling procedure based on one of these seems appropriate for general considerations. All parameters of interest are shown in relation to those of the reference design.

2.1 Plasma scaling

The β-scaling generally used to-day is

$$\frac{\beta}{\beta_o} = \frac{g\,(1+k^2)\,q_o\,A_o}{g_o(1+k_o^2)\,q\,A} = \frac{n\,T}{n_o T_o}\left(\frac{B_o}{B}\right)^2 = \frac{n}{n_o}\,\vartheta\,\left(\frac{B_o}{B}\right)^2 \tag{1}$$

This yields for the poloidal beta

$$\frac{\beta_{pol}}{\beta_{pol_o}} = \frac{g\,q\,A}{g_o q_o A_o} \tag{2}$$

The following abbreviation proves to be practical

$$M = \frac{g_o(1 + k^2)\, q_o}{g\ (1 + k_o^2)\, q} \tag{3}$$

The range of validity of the ß-scaling experimentally verified so far extends up to k = 1.6. It is assumed here that this range of validity could expand up to about 2.3. Appropriate experiments are under preparation (e.g. Big Dee with A = 2.5). Constraints for a practical configuration may limit k to about 2.

The following abbreviations are used:

for the reactor power (thermal) $P/P_o = \eta$ (4)

for the major radius $R/R_o = \rho$ (5)

for the wall loading (neutrons) $p_w/p_{wo} = \delta$ (6)

for the performance parameter (confinement time prop. to current) $\gamma = \frac{n\ \tau_E}{n_o \tau_{Eo}}$ (7)

Average plasma data are used (n; $T_e = T_i = T$), it being assumed that the profiles of the reference design apply.

After some intermediate evaluation one obtains the following relations:

plasma current
$$\frac{I}{I_o} = \left[\frac{\eta^2\ M^3}{\gamma\ \vartheta}\ (\frac{k_o}{k})^2\right]^{1/5} \cdot \frac{A_o}{A} \tag{8}$$

minor plasma radius
$$\frac{a}{a_o} = \left[\frac{\eta^3\ M^2}{(\gamma\ \vartheta)^4}\ (\frac{k_o}{k})^3\right]^{1/5} \cdot \frac{A_o}{A} \tag{9}$$

and hence

major plasma radius
$$\rho = \left[\frac{\eta^3\ M^2}{(\gamma\ \vartheta)^4}\ (\frac{k_o}{k})^3\right]^{1/5} \tag{9a}$$

poloidal flux (approx.) $$\frac{I\,R}{I_o R_o} = \frac{\eta\,M}{\gamma\,\vartheta}\,\frac{k_o}{k}\,\frac{A_o}{A} \qquad (10)$$

toroidal field (on axis) $$\frac{B}{B_o} = \left[\frac{(\gamma\,\vartheta)^3}{\eta\,M^4}\,\frac{k}{k_o}\right]^{1/5} \cdot \frac{g_o A}{g\,A_o} \qquad (11)$$

wall loading $$\delta = \left[\frac{(\gamma\,\vartheta)^3}{\eta\,M^4}\,\frac{k}{k_o}\right]^{1/5} \cdot \gamma\,\vartheta\,\frac{A\,k}{A_o k_o}\left[\frac{1+k_o^2}{1+k^2}\right]^{1/2} \qquad (12)$$

Comparison with eq. (11) yields as an alternative

$$\delta = \gamma\,\vartheta\,\frac{g\,B\,k}{g_o B_o k_o}\left[\frac{1+k_o^2}{1+k^2}\right]^{1/2} \qquad (13)$$

The plasma density is $$\frac{n}{n_o} = \frac{I_o}{I}\,\gamma \quad (\tau_E \sim I). \qquad (14)$$

Further one obtains the Murakami parameter with eqs. (1), (9a) and (11)

$$\frac{n\,R\,B_o}{n_o R_o B} = m \geqq \frac{g\,I\,A}{\vartheta\,g_o I_o A_o} \qquad (15)$$

According to the usual representation, the density limit is described by a straight line passing through the origin in the coordinate system of inverse safety factor vs. the Murakami parameter. If the influence of further parameters is neglected this yields the condition at the density limit (on the assumption that the ratio of the current-q values is equal to the ratio of the boundary-q values):

$$m \leqq \frac{q_o}{q} \qquad (15a)$$

All essential data are thus now available as functions of the relative power, aspect ratio, elongation, safety factor, g-factor of the ß-scaling, performance parameter, and plasma temperature.

In order to tell, however, what reactor configurations are possible in practice, the conditions of a consistent geometry have to be considered as well. For the above equations they provide the value of the aspect ratio, which cannot be chosen arbitrarily.

2.2 Geometric-electromagnetic-nuclear scaling

This part of the scaling ensures that the practical configuration assumed is compatible with the provision of a sufficient magnetic flux swing appropriate to the respective plasma current and with the shielding thickness appropriate to the respective wall loading.

There is no limitation to the degree of detail in iteratively evaluating a practical configuration. For the investigations here it is sufficient to assume the flux swing to be proportional to I.R, which is fulfilled quite well if $A/A_o \cdot \sqrt{k_o/k}$ remains close to 1. (Otherwise a correction of the flux density swing may serve for adjustment.) The shielding thickness is a part of the input.

A first geometrical condition for the aspect ratio is thus obtained

$$\frac{A}{A_o} = f_1 \left(\Delta B/\Delta B_o ; \eta ; \gamma \vartheta ; M \right) \tag{16}$$

Since the performance parameter depends on a consistent data set, a second geometrical condition has to be used. It is required that in the configuration defined by A/A_o the actual toroidal field be identical to that already given by eq. (11). For this purpose the geometry dependence of the field is represented in the following form:

$$\frac{B}{B_o} = f_2 \left(\Delta B/\Delta B_o ; \eta ; \gamma \vartheta ; M ; A/A_o \right) \tag{17}$$

and is equated with eq. (11) iteratively.

Taking the shielding thickness appropriate to the wall loading considered, one gets eqs. (16) and (17) in the form

$$\frac{A}{A_o} = E \left[\frac{\Delta B_o I R}{\Delta B\ I_o R_o}\right]^{1/2} \frac{a_o}{a} + F + G \frac{a_o}{a} \qquad (18)$$

$$\frac{B}{B_o} = \frac{\rho}{E + H} \left(E \left[\frac{\Delta B_o I R}{\Delta B\ I_o R_o}\right]^{1/2} + H \right) \qquad (19)$$

Equation (19) implies that the maximum toroidal field of the reference design is retained.

The values of the factors E, F, G, H differ somewhat for different reactor designs. Table 1 shows the values for INTOR and STARFIRE /2/.

Table 1: Geometry factors

	E	F	G	H
INTOR	0.447	0.283	0.270	0.081
STARFIRE	0.457	0.306	0.237	0.066

3. Results

3.1 Orienting evaluation for INTOR

First rescaling calculations for orientation were carried out on the basis of the INTOR parameter set in the range $0.6 \leqq g/g_0 \leqq 0.7$ with $\delta = 1$ kept constant. (The wall loading is a test parameter for INTOR and should be achieved with reasonable outlay, i.e. with limited reactor power, plasma current and dimensions.)

In the sense of the β-scaling now used the factor g assumed so far for INTOR is too large (as in the case of many other tokamak reactor designs). It is found that with $k/k_0 = 1$ ($k_0 = 1.6$) reductions in g/g_0 have to be compensated with considerable increases in outlay. An increase in elongation to $k = 2$ ($k/k_0 = 1.25$) again reduces the outlay but still leaves it above the original level (for g/g_0 between 0.6 and 0.7 as applied to INTOR, which seems possible with $g_0 = 5.67$. A reduction of the alpha and impurity contributions to the INTOR reference beta by 0.5% would yield $g_0 = 5.16$). Roughly speaking, with an elongation of 1.6 one has double the power and plasma current, while with an elongation of 2 a 20% higher power and a 40% higher plasma current are typical examples (see Figs. 1 and 2). An increase of the flux density swing rather has a negative impact because the maximum toroidal field cannot be increased at the same time (see Figs. 3 and 4).

If the Murakami parameter is taken to be the same as in INTOR, one has $m = 1$ and $q/q_0 = 1$ at the density limit. With $\vartheta = 1$ it can immediately be seen from eq. (15) that the beta scaling proportional to the plasma current adversely affects the ability to adhere to the density limit. (For the possibility of increasing the respective margin by raising the temperature see Sec. 3.2.3.)

A check on the data in Figs. 1 and 2 using eq. (15) ($m = 1$) shows that for $k/k_0 = 1$ the density limit is just violated, while for $k/k_0 = 1.25$ it is adhered to with a small margin to spare. Taking adherence to the density limit for k/k_0 = 1.25 as a condition, one gets curves which constitute upper limits for the power and the wall loading under the assumptions made. The achievable wall loading remains almost constant over the range considered (Fig. 5).

3.2 Parameter studies

Below are a number of parameter studies that can provide an overview on consequences and possible remedies facing the somewhat less favourable ß-scaling compared with previous assumptions.

3.2.1 INTOR alternatives with minimum increase in outlay

The simplified scaling relations can be used to find parameter ranges affording interesting INTOR alternatives with minimum increase in outlay. As an example one obtains for the condition $\beta/\beta_0 \cdot A/A_0 = 1$ and for $\eta = 1$ data sets for INTOR alternatives that closely approximate the major radius of INTOR. The impact of decreasing values of g/g_0 between 0.7 and 0.6 is compensated to a certain degree by an increase in elongation ($q/q_0 = 1$). Figure 6 shows the various reactor parameters versus elongation this being the strongest modifying influence. The curves show very clearly the gap between the existing reference point for INTOR and possible alternative data sets. Depending on the elongation chosen, the data set used hitherto is "fanned" out, some of the parameters deviating considerably from their initial values. The effect of the more or less well-defined ß-limit is shown in Fig. 6 in two ways. Firstly, the values of β/β_0 that appear to be possible in practice are shown. Secondly, curves derived from fitted scaling formulae obtained by Tuda et al /3/ and Bernard et al. /4/ by means of MHD calculations are added. These curves relate to the so-called $n = \infty$ ballooning instability as one reason considered for the ß-limit. The crossover points of these theoretical curves with the curve representing feasible reactor configurations indicate a certain safety margin for g/g_0 between 0.7 and 0.6, albeit a rather small one. The two theoretical ß-limits show a somewhat different behaviour; nevertheless their above-mentioned crossover points indicate clearly an upper boundary area between accessible and inaccessible data sets for INTOR alternatives. The $n = 1$ kink limit on beta would shift this boundary to even larger elongation. See also Sec. 3.2.2. (For the calculation of the theoretical ß-values the triangularity is assumed to be 0.3, as for INTOR.)

If one discards the condition $q/q_0 = 1$ used so far, the necessary increase in elongation can be reduced for smaller q-values (which might be permissible on the basis of experimental results, though $q < 2$ has so far only been reached in the limiter configuration). As shown in Fig. 6, e.g. for $g/g_0 = 0.65$, both the major radius and the wall loading (at $\eta = 1$) can be brought to the INTOR values. The values of g/g_0 and k/k_0 are 0.89 and 1.29, respectively. The density limit is not reached.

3.2.2 INTOR alternatives with $\eta = 1$, $\delta = 1$, $\rho = 1$

The example described in Sec. 3.2.1 suggests looking more generally for those alternatives which in the accessible range of g/g_0 have the same power, the same wall loading and the same major radius as the reference design. For such alternatives q/q_0 and k/k_0 are prescribed accordingly.

One obtains after some intermediate evaluation the following relations:

Plasma current $$\frac{I}{I_0} = \left[\frac{g_0 q_0}{g\, q}\right]^{1/2} \left[\frac{k_0}{k}\right]^{1/4} \tag{20}$$

The plasma current increases by about $\sqrt{g_0/g}$, e.g. with $g/g_0 = 0.65$ by a factor of about 1.2 for $q/q_0 = 1$.

Minor radius, aspect ratio $$\frac{a}{a_0} = \frac{A_0}{A} = \left[\frac{1 + k_0^2}{1 + k^2}\right]^{1/2} \tag{21}$$

The minor radius reduction contributes essentally to the cross section elongation. The vertical minor radius thus may not have to become much larger.

Toroidal field on axis $$\frac{B}{B_0} = \left[\frac{g_0 q}{g\, q_0}\right]^{1/2} \left[\frac{k_0}{k}\right]^{1/4} = \frac{q\, I}{q_0 I_0} \tag{22}$$

The increase in aspect ratio causes an increase of the toroidal field on axis for a constant maximum field.

Beta value $$\frac{\beta}{\beta_o} = \frac{g\,q_o}{g_o q} \left[\frac{1 + k^2}{1 + k_o^2}\right]^{1/2} \qquad (23)$$

The reduction in g/g_o is partially compensated for by increasing k/k_o and lowering q/q_o. The plasma power density increases by a factor of $(1 + k^2)\ k_o\ /\ (1 + k_o^2)\ k$.

Poloidal beta $$\frac{\beta_{pol}}{\beta_{pol_o}} = \frac{g\,q}{g_o q_o} \left[\frac{1 + k^2}{1 + k_o^2}\right]^{1/2} \qquad (24)$$

A compensation similar as for β is not possible for β_{pol}.

Plasma density $$\frac{n}{n_o} = \left[\frac{k_o}{k}\,\frac{1 + k^2}{1 + k_o^2}\right]^{1/2} \quad \text{with} \quad \gamma = M^{1/2} \cdot \left(\frac{k_o}{k}\right)^{3/4} \qquad (25)$$

The density is somewhat larger than in the reference design. ($\vartheta = 1$)

Murakami parameter $$m = \left[\frac{g\,q_o}{g_o q}\,\frac{1 + k^2}{1 + k_o^2}\right]^{1/2} \left[\frac{k_o}{k}\right]^{1/4} \qquad (26)$$

In general, the Murakami parameter is somewhat smaller than in the reference case, i.e. the alternatives considered in this section are somewhat more favourable with respect to the density limit compared with the reference. Since eq. (21) already defines the aspect ratio in terms of k/k_o, the two geometry relations (18) and (19) reduce to one equation for the toroidal field which determines the relation between k/k_o and q/q_o when it is equated with eq. (22) and eq. (20) is inserted:

$$\frac{B}{B_o} = \frac{E\,\left(\frac{I}{I_o}\right)^{1/2} + H}{E + H} \qquad (27)$$

$\Delta B/\Delta B_o = 1$ is implied. (For more details see Annex 1.)

Figure 7 shows data for INTOR alternatives with $\eta = \delta = \rho = 1$. In the range covered, with g/g_0 between 0.7 and 0.6, the axial toroidal field and the vertical minor plasma radius remain nearly constant, and the plasma current is about 20 to 30% larger than for INTOR. ß-values of up to 90% of the INTOR value are achieved. The safety factor at the plasma boundary, q_s, calculated with the formula of Tuda et al. /3/, appears to be far enough from the lower limit of 2. β_{pol} only reaches about 70% of the INTOR value. The aspect ratio is above 5, the increased elongation being attained mainly by reducing the horizontal plasma radius. In addition to the ballooning beta limits, the curve for the n = 1 kink limit of Tsunematsu /5/ is also shown here. This limit is always surpassed with the present kind of design, except for $g < 3.5$ ($g_0 = 5.67$). For alternative data based on $g_0 = 5.16$ see Annex 2. Annex 3 lists formulae for theoretical ß-limits.

The almost constant value of the toroidal field in Fig. 7 suggests considering a single design which has, for example, the data for $k/k_0 = 1.23$ (Fig. 7, left boundary of the range considered), but also approximately covers the operating data for the larger elongations (up to the right-hand boundary of the range), i.e. that can be adjusted to g/g_0 values of between 0.7 and 0.6.

The result of such a parameter rescaling is shown in Fig. 8. The main difference to Fig. 7 is that - since only one machine is now involved - the power and the wall loading decrease as g/g_0 decreases. While ß remains constant, g/g_0 decreases somewhat more strongly than in Fig. 7 in keeping with the plasma current in one and the same configuration. The current increase also causes an increase of the flux density swing by up to 7%.

Figure 9 indicates the modifications in machine geometry of the alternative in Fig. 8 on the basis of the radial dimensions and also the plasma cross-sections. Accordingly, one could manage with rather modest machine modification.

If the assumptions for the increase of k and the decrease of q are taken to be permissible, it thus appears possible to define INTOR alternatives that adhere to the power data and the major radius of INTOR and take into account the ß-scaling now observed. The data sets are somewhat more favourable than INTOR with respect to both the density limit and the performance parameter (with a scaling of the energy confinement time proportional to the plasma current). Since attractive INTOR alternatives are thus possible, but, on the other hand, some parameter dependences - especially in a future reactor regime - are only rather roughly known, it does not seem very appropriate at this time to alter the INTOR concept drastically.

With the data shown in Fig. 8 the modifications are limited to

- increase of the plasma current by up to 28% (which has consequences for the poloidal field system, including position control, due to larger elongation, for the support structure, and for current disruption effects);
- increased elongation of the plasma cross-section up to about k = 2.15 (which has consequences for the wall configuration, the divertor geometry - provided the beta limits are not only achieved in the limiter case, as was seen in Doublet III - and for the toroidal field coil size and shape together with their impact on the poloidal field coil system) at a somewhat reduced safety factor;
- a somewhat increased flux density swing in the central solenoid when the range down to $g/g_0 = 0.6$ has to be covered with an INTOR alternative designed for $g/g_0 = 0.7$.

The total outlay for an INTOR alternative bounded in such a manner should not be very much larger than that estimated so far for INTOR, the slowing down of the plasma current scenario perhaps affording a possible compensation.

3.2.3 Rescaling in a wider power range taking into account the density limit.

Taking m = 1 as an additional condition for rescaling INTOR, one obtains for $q/q_0 = 1$ (density limit) INTOR alternatives in which the power, the wall loading and the major radius are no longer simultaneously equal to those in INTOR. These alternatives tend to be larger than INTOR at the same wall loading (but manage with a somewhat smaller elongation than the previous alternatives) or they reach a somewhat larger wall loading than INTOR if they are closer to INTOR in geometry or power as a result of increased elongation.

Figure 10 shows some possible data sets for $\delta \approx 1$ which are subsets from the more general chart in Fig. 11. Conceptual designs based on the scaling relations shown in Sec. 2.1 - irrespective of the geometry iteration in Sec. 2.2 that is needed for determining feasible values of the radius, plasma current, magnetic field, density, etc. - exhibit the following characteristic formula (independent of the confinement scaling):

$$\eta\rho = (m\vartheta)^4 \cdot \left(\frac{g_0 q}{g\, q_0} \frac{1 + k_0^2}{1 + k^2} \right)^2 \cdot \frac{k}{k_0} = (m\vartheta)^4 \left(\frac{\beta_0 A_0}{\beta A} \right)^2 \cdot \frac{k}{k_0} \qquad (28)$$

The product of the reactor power and major plasma radius, i.e. the reactor size, is essentially governed by, besides beta, the product of the Murakami parameter and the temperature. If $m < q_0/q$, the density limit is not reached. If one has to put $m < 1$ because too high a value of the Murakami parameter was assumed in the reference design, some compensation with respect to reactor size can be achieved - within certain limits - by raising the assumed plasma temperature.

Figure 11 shows curves according to eq. (28) for three values of g/g_0 and two values of q/q_0 versus elongation. (For $q/q_0 = 1$, $m = 1$ the corresponding designs are at the density limit; for $q/q_0 = 0.85$, $m = 1$ they do not reach the density limit.) Curves for constant parameter values of A/A_0, δ, I/I_0 and ρ are included in the families of curves for $q/q_0 = 1$ and 0.85, relating to the INTOR configuration. It is found that for the entire range covered the wall loading possible is fixed within rather narrow limits. The impact of individual plasma parameters on the outlay is clearly seen. The smallest possible current increase relative to INTOR is about 1.25, this being true for a large range in the vicinity of $\eta \cdot \rho = 1$. Alternatives retaining the original elongation $k_0 = 1.6$ involve strong increases in outlay. The aspect ratio is $A/A_0 > 1$ almost everywhere. For the data of Fig. 11 the value of the performance parameter is $\gamma > 1$. The above-mentioned possibility of compensating $m < 1$ by raising the temperature is restricted when, for example, with a given value of $\gamma \cdot \vartheta$ and with $\vartheta > 1$ the value of γ reduces to 1. If it is assumed that $kT_0 = 10$ keV, the principal range of variation in the context of this simplified rescaling is with sufficient accuracy $1 \leq \vartheta \leq 2$. This variation range can be restricted because of the condition $\gamma \geq 1$. In order to open up the parameter range also for successors to INTOR with much higher wall loading (if feasible), the product $m \cdot \vartheta$ has to be increased above the value assumed for INTOR.

Figure 12 shows parameters for $m = 1$, $\vartheta = 1.5$ as represented in Fig. 11. The inner shield thickness is assumed to be the same as in INTOR although now one has $\delta \approx 2$ in the entire range considered. This assumption is sufficiently accurate for orientation and leaves open the possibility that such configurations can also be achieved with a somewhat thicker shield but a reduced fraction of inductive current drive, or that more efficient shielding material would be applied and/or the shielding requirements could be lowered. Figure 11 also shows that a reactor scaled up form INTOR at about $\eta \cdot \rho = 6.8$ with $m = 1$, $\vartheta = 1.5$, $g/g_0 = 0.65$ could have a major radius a factor of 1.4 larger than in INTOR, more than twice the current of INTOR, an aspect ratio of almost 5, and a wall loading of about 2.7 MW/m^2. (When comparing such figures with those for the STARFIRE alternatives shown below, one should also note the difference in reference configurations. One important difference is the much larger relative plasma-wall distance on the inside in INTOR.)

Another way of representing the scaling is shown in Figs. 13 and 14. Here the essential reactor parameters are given vs. $m \cdot \vartheta$ for fixed pairs of q/q_0 and k/k_0 and for $g/g_0 = 0.7$ and 0.6, with INTOR as reference. It is found that variation in the input figures for g/g_0, q/q_0 and k/k_0 leads to a kind of parallel shift of the curves, the exponential dependence of the individual quantities on $m \cdot \vartheta$ being fixed as follows:

$$\eta \sim (m\vartheta)^{3.25}$$
$$\delta \sim (m\vartheta)^{1.67}$$
$$I/I_0 \sim (m\vartheta)^{1.15}$$

Because of eqs. (8), (15) and (28) the following relations also hold on the average:

$$\rho \sim (m\vartheta)^{0.75}$$
$$A/A_0 \sim (m\vartheta)^{-0.15}$$

The exponents result in detail from the reference geometry derived from the geometry factors of Table 1. Hence Fig. 15 shows a further set of curves relating to STARFIRE as reference. A slight increase in the exponents can be seen. The values of g/g_0 and q/q_0 chosen in Fig. 15 are such that g becomes about 3.7 and q about 2. With the elongation selected, one could combine the values of the reactor power, wall loading and major radius almost exactly as in STARFIRE; the plasma current still has to be raised by 44%. Despite the 15% lower ß-value, the plasma power density is higher than that in the reference design as a result of the aspect ratio being increased to about 5 and the associated larger toroidal field on axis with a fixed maximum field. Since both the stable operation of highly elongated plasmas and the validity of the ß-scaling are still open questions for such plasmas, Fig. 16 finishes by giving curves for the essential reactor parameters of STARFIRE alternatives with $\eta = 1$ versus elongation. The same value of the Murakami parameter has been assumed as for INTOR. This figure also clearly shows the marked influence of the elongation on the outlay.

4. Summary

The foregoing study yields the following conclusions:

- The ß-scaling in the range $(3.5 - 4) \cdot I / a \cdot B$, when applied to possible INTOR alternatives, leads to a 2.5-1.8-fold reactor power and a 2.2-1.7-fold plasma current for alternatives retaining the elongation and wall loading of INTOR.

- An increase in elongation (if possible and as effective for ß as assumed here) of up to 2 could bring these figures down to 1.4-1.1-fold for the power and to 1.6-1.3-fold for the current. Accordingly an even greater elongation could further improve the situation.

- The performance parameter γ is higher than that of the reference case because of the scaling for the energy confinement time in proportion to the plasma current.

- If the Murakami parameter assumed for INTOR proves to be too large, an increase of the specified plasma temperature could provide for compensation with respect to reactor size.

- An example shown here (see Fig. 8) presents an INTOR alternative that has the same radius, the same wall loading and the same power as INTOR. According to the g-value of the β-scaling the elongation required is up to 2.17, the minimum current-q is 1.71, and β reaches 5.1%. At the same time the current rises to up to 8.2 MA, i.e. a 1.28-fold increase. (The "reserves" contained in the INTOR data set with respect to the relative alpha and impurity contributions to beta have been taken over without change. See Annex 2, however, where the "reserves" are partially used for improvement.)

- Since some detailed scaling relations, especially for a future reactor regime, are as yet only approximately known, it does not seem appropriate at present to change the INTOR concept drastically beyond the extent specified in Fig. 8. An essential increase in elongation and an increase in current, however, are unavoidable if the defined objective is to remain unchanged and the outlay is not to be considerably increased. A certain increase in outlay is still needed to increase the current.

- The application of the scaling relations to STARFIRE as an example of a later successor to INTOR also yields the possibility of defining a STARFIRE alternative having the same power, wall loading and major radius as in the reference design. It is necessary, however, to increase the elongation to 2.28 and to lower the safety factor (current-q) to 2. Hence the Murakami parameter rises to a value such as assumed for INTOR. (The possibility of compensation by raising the plasma temperature would be restricted, since it has already been applied in the STARFIRE reference design.) The current increase here amounts to 44%.

- The demanding requirements deriving from these data suggest the need for considering innovative concepts.

References

/1/ INTOR Phase Two A Part 1 report, IAEA Vienna 1983, STI/PUB/638 and INTOR workshop Vienna October 1984.

/2/ STARFIRE, ANL/FPP -80-1 (Argonne, September 1980)

/3/ T. Tuda et al.: IAEA conference London 1984, paper CN-44/E-III-4

/4/ L.C. Bernard et al.: Nuclear Fusion 23 (1983), p. 1475

/5/ S. Tokuda et al.: JAERI-M 9899 (1982)

ANNEXES 1 - 3

Annex 1: Elongation and density limit vs. safety factor (INTOR rescaling).

The evaluation of eqs. (26) and (27) yields the dependence of elongation vs. reduced safety factor together with the Murakami parameter, the density limit being represented by eq. (15a).

It is found that an increase in elongation e.g. in a range between 1 and 1.4 (k_o = 1.6) is associated with a reduction of the safety factor of between 0.82 and 0.93 depending on g/g_o in a range between 0.6 and 0.7, if the condition $\eta = \delta = \rho = 1$ is to be kept. Within these limits the relative Murakami parameter is always below the density limit given by q_o/q ($\vartheta = 1$), as shown in Fig. A1.

Annex 2: Impact of g_o on location of ß-limit when rescaling INTOR.

The INTOR reference design assumes a total β_o = 5.6% of which 4.1% is the D-T contribution essential for the reactor power figures. The rest is attributable to alpha and impurity pressure. If it would be possible to reduce these contributions such that with a constant D-T contribution the total beta would amount to e.g. 5.1%, g_o would become 5.16 (instead of 5.67).

The impact of such an improvement is shown in Fig. A2 which is a modified version of Fig. 7. It is found that with g_o = 5.16 even the theoretical n = 1 kink beta limit /5/ is fulfilled, at least at the right hand boundary of the parameter range considered. This range now refers to g-values between 3.6 and 3.2.

Annex 3: Formulae used for theoretical ß-limit

Ballooning limit of Tuda et al. /3/

$$\beta = \frac{30k^{1.5}}{Aq_s}\left[1+0.9(k-1)\Delta-0.6\frac{k^{0.75}}{q_s}+14(k-1)(1.85-k)\frac{\Delta^{1.5}}{q_s^4}\right] \ \%$$

$$\frac{1}{q_s} = A\sqrt{1-\frac{1}{A^2}}\left(\frac{2}{1+k^2}-0.08\,\Delta\right)\frac{\mu_o I}{2\pi aB}-0.07\left[1+(k-1)\Delta\right] \quad (\Delta = \text{triangularity})$$

Ballooning limit of Bernard et al. /4/

$$\beta = \frac{27k^{1.2}(1+1.5\,\Delta)}{A^{1.3}q^{1.1}} \ \% \qquad \text{(current-q used for evaluation)}$$

Kink limit of Tsunematsu (see Tokuda et al. /5/)

$$\beta = \frac{14k^{1.56}}{Aq_s}\left[1+(k-1)\,\Delta\right] \ \% \qquad (2 < q_s < 3), \qquad q_s \text{ definition as above}$$

The symbols have the same explanation as used in Sec. 2.

Possible INTOR alternatives (data for orientation)

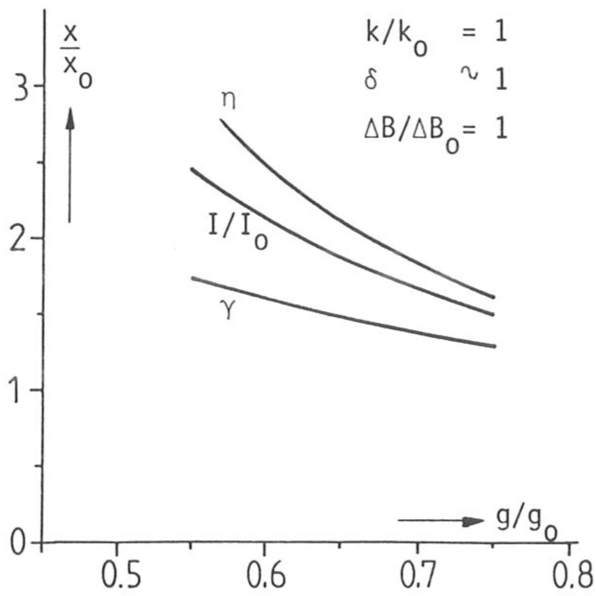

Fig. 1

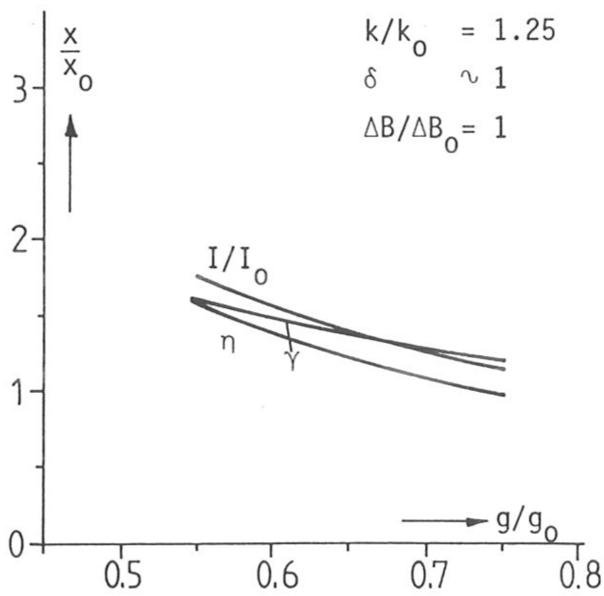

Fig. 2

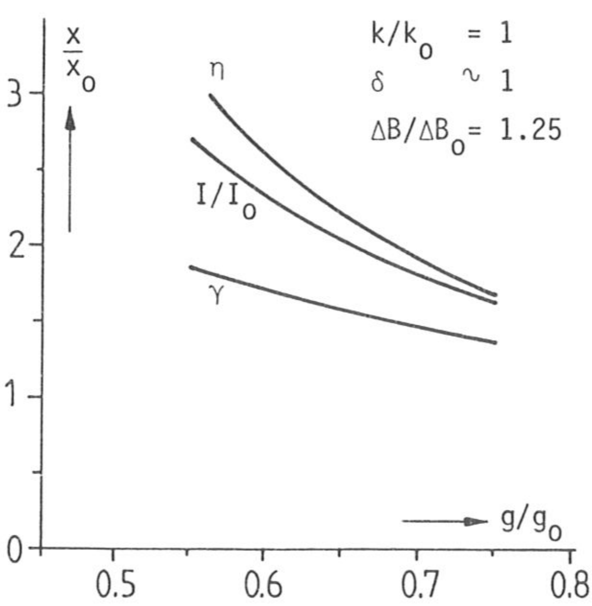

Fig. 3

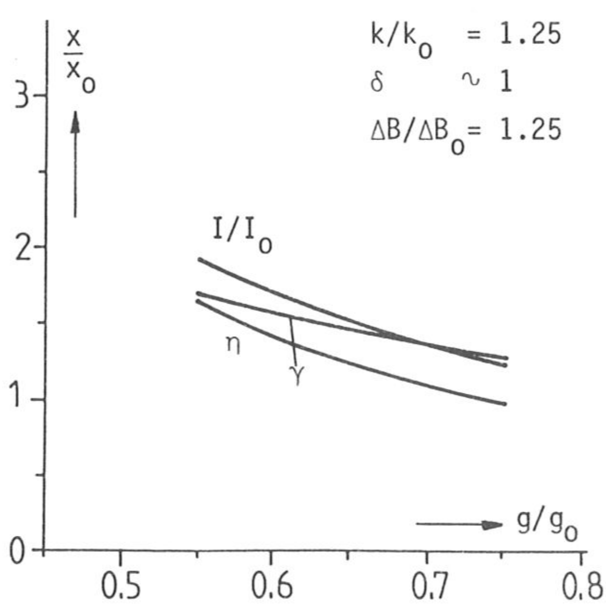

Fig. 4

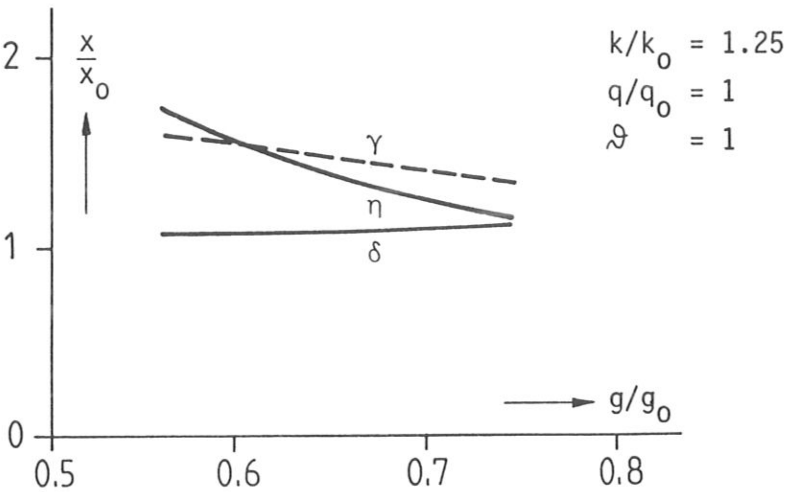

Fig. 5: INTOR alternatives for m = 1

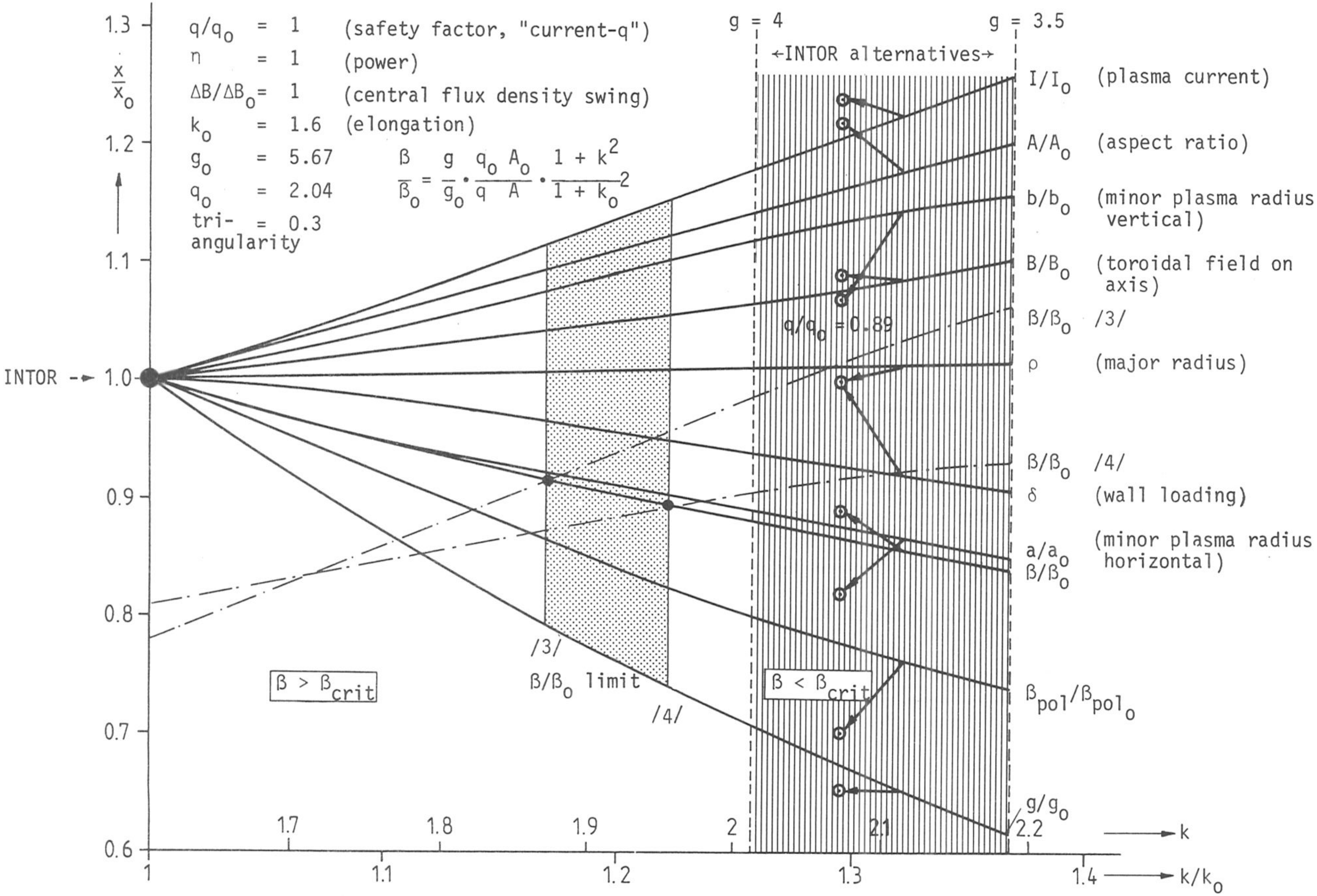

Fig. 6: INTOR rescaling for constant reactor power and approximately constant geometry

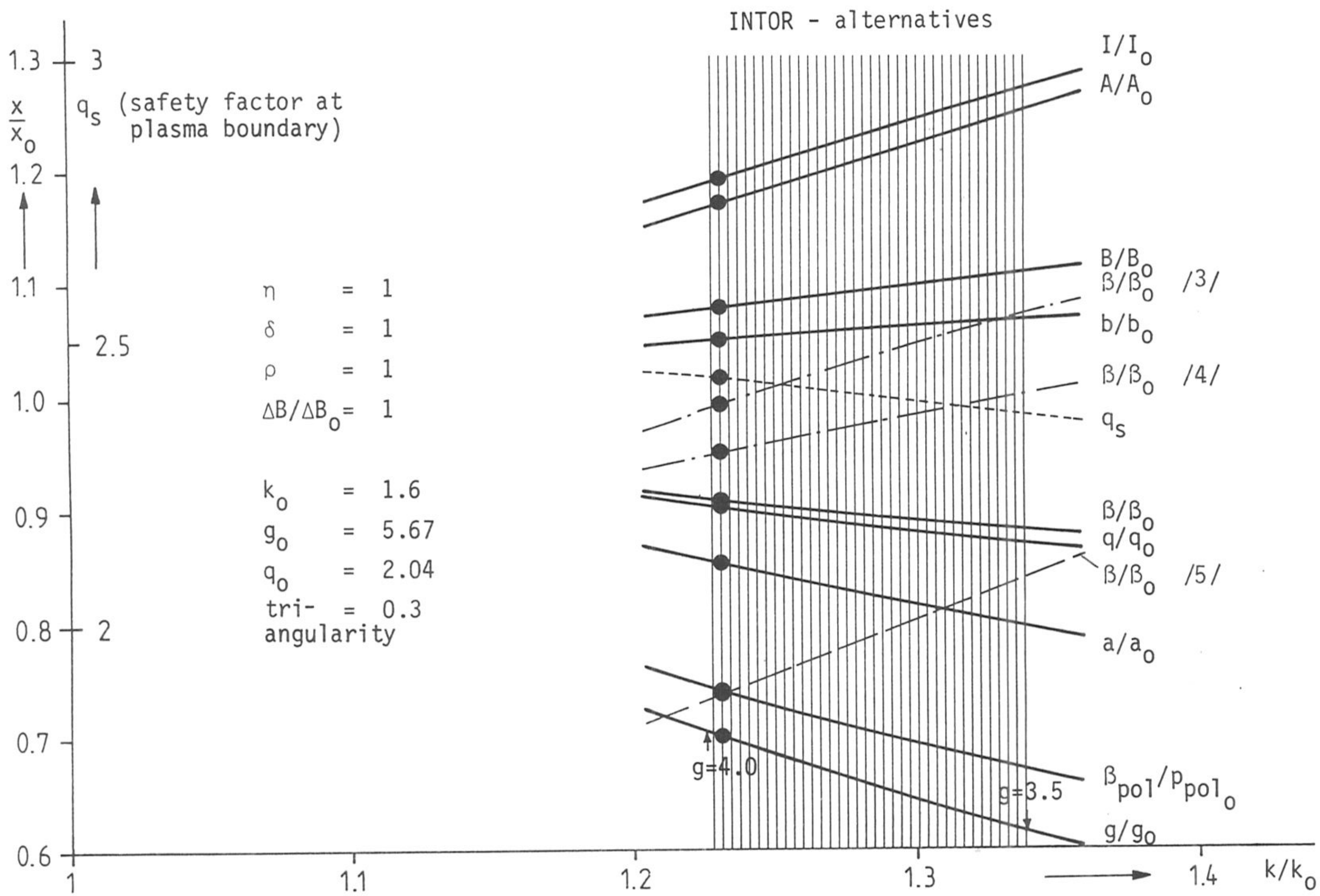

Fig. 7: <u>INTOR rescaling for $\eta = \delta = \rho = 1$</u>

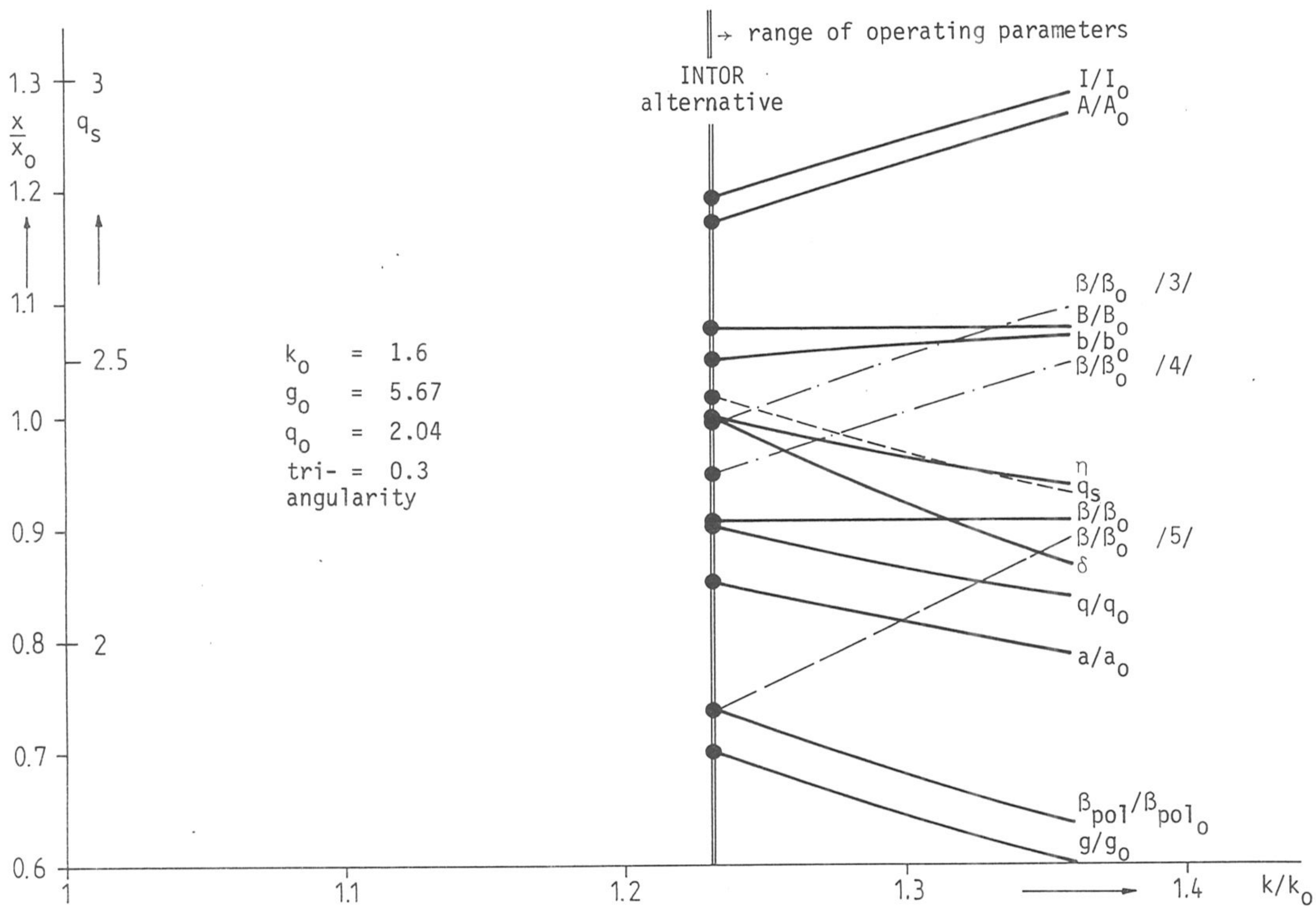

Fig. 8: INTOR rescaling for constant toroidal field on axis and $\rho = 1$

Fig. 9: Geometry modification with $\rho = 1$

1. Radial build

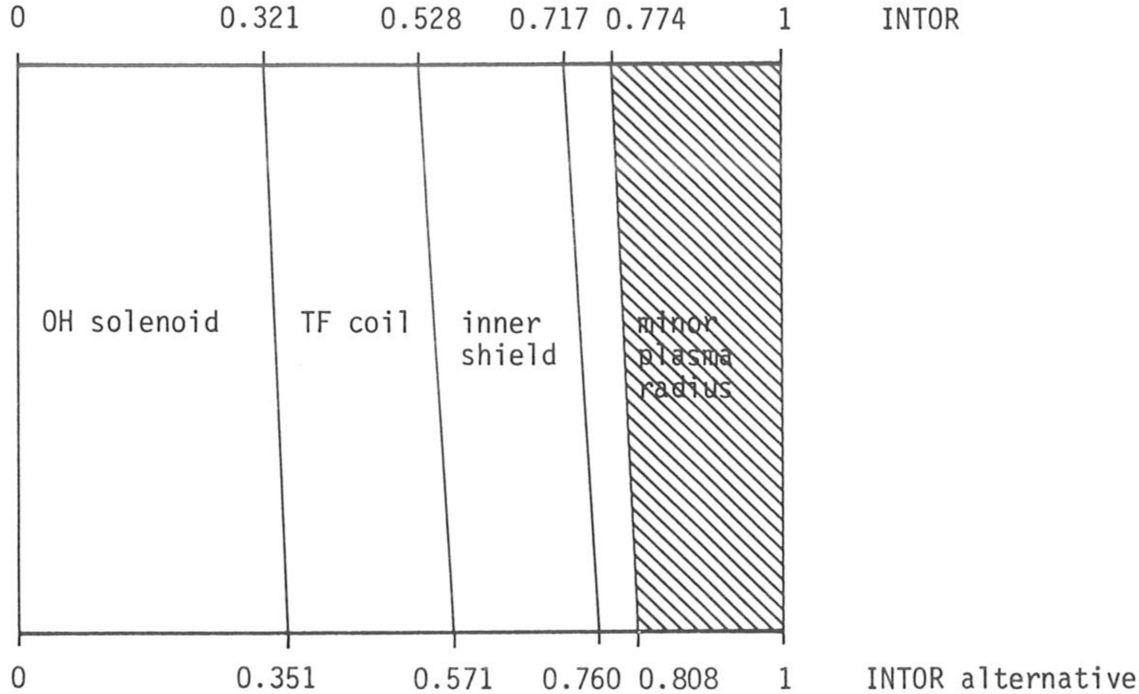

2. Plasma cross section

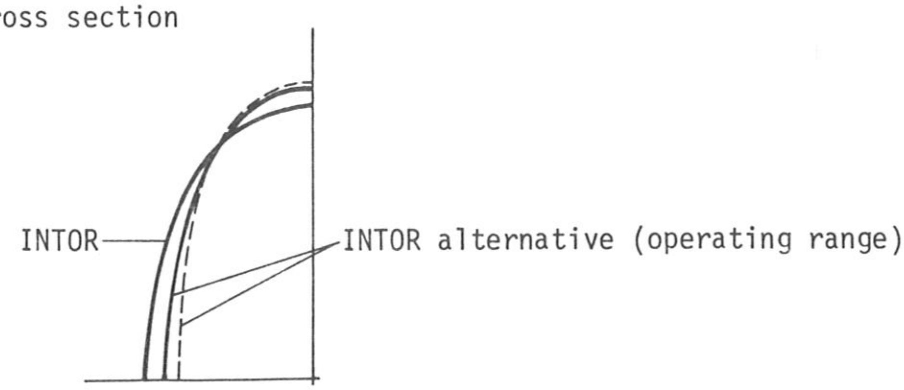

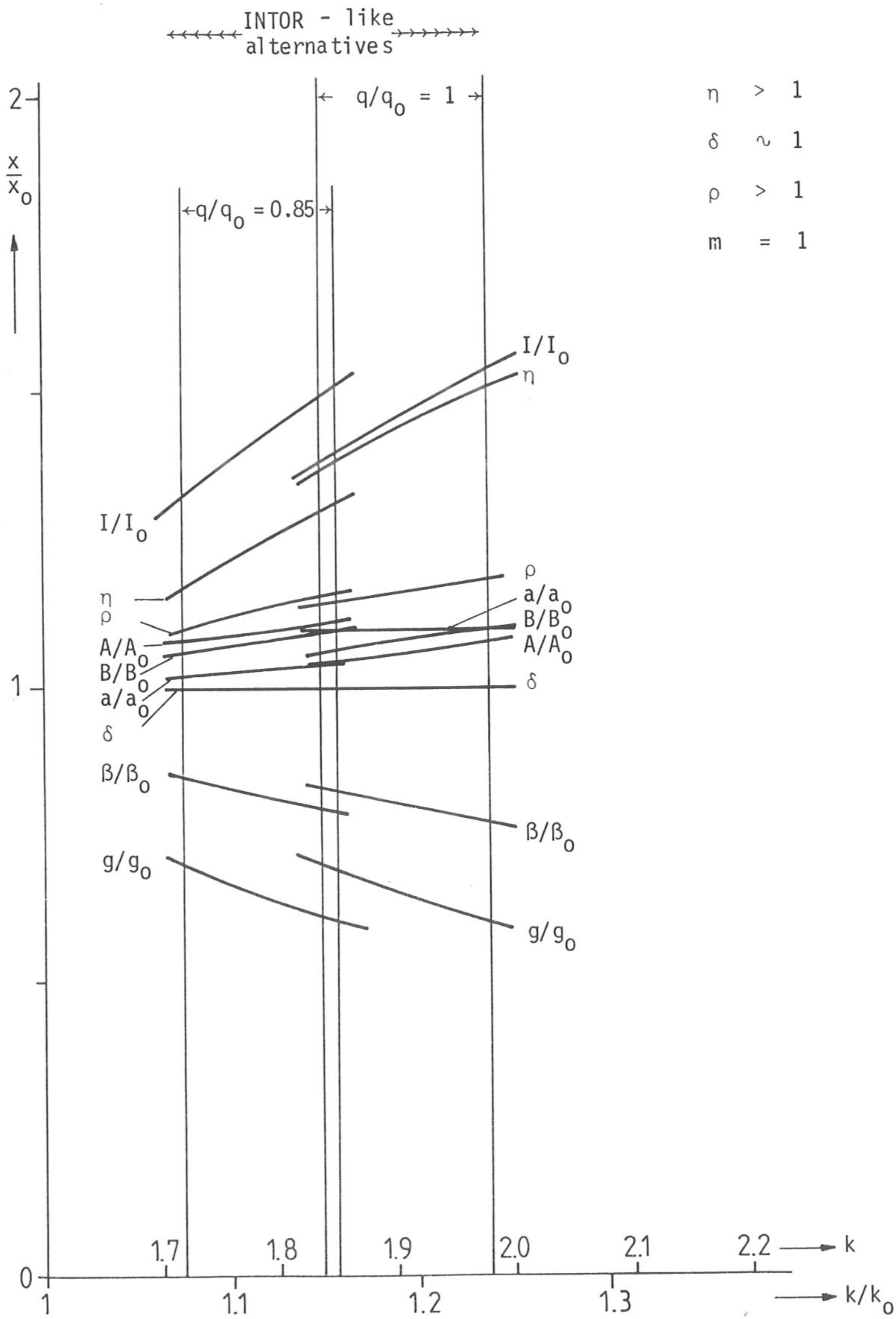

Fig. 10: INTOR-like alternatives for m = 1 with larger dimensions and larger power

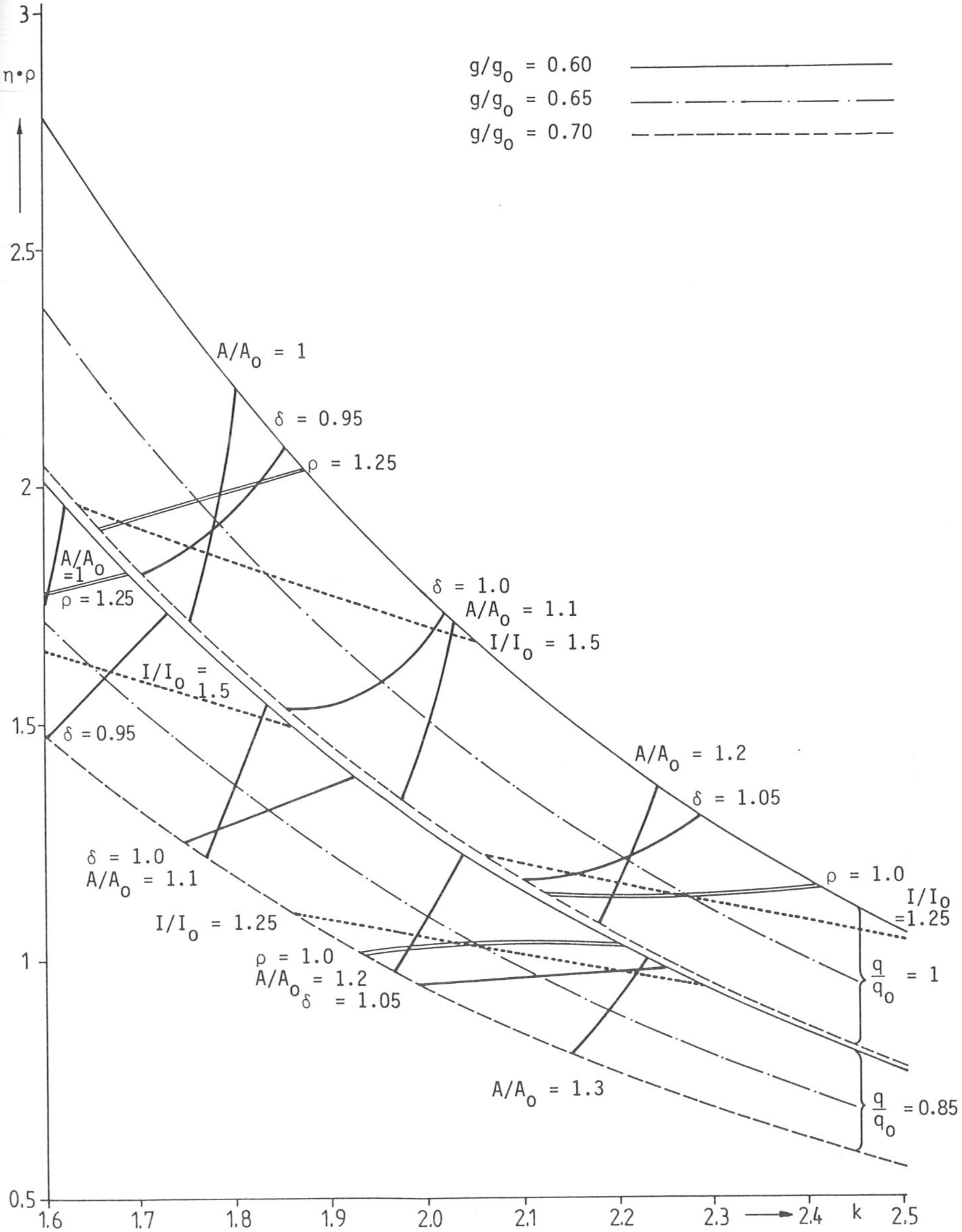

Fig. 11: INTOR alternatives in a wider parameter range for $m \cdot \vartheta = 1$

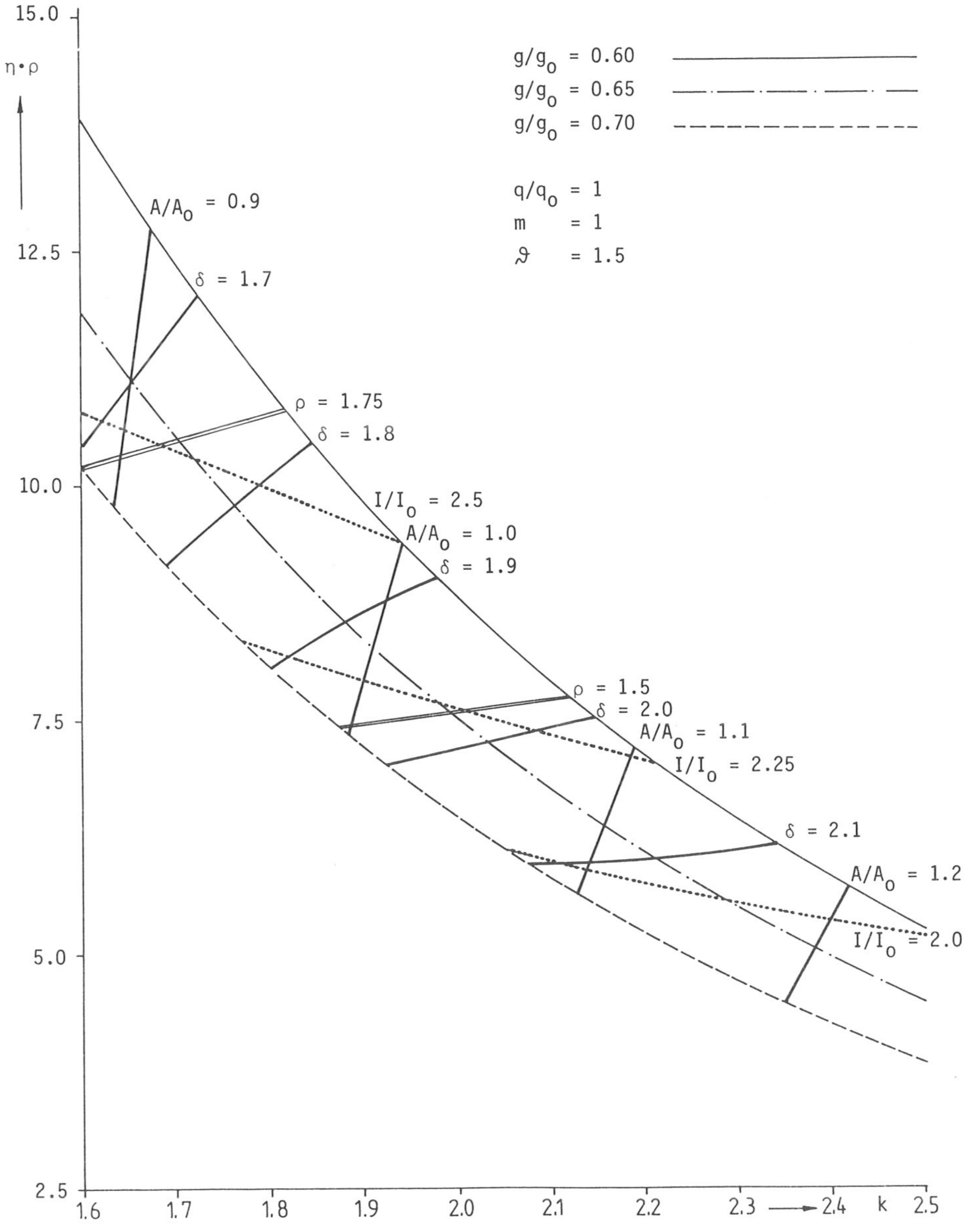

Fig. 12: Reactor scaling based on the INTOR configuration

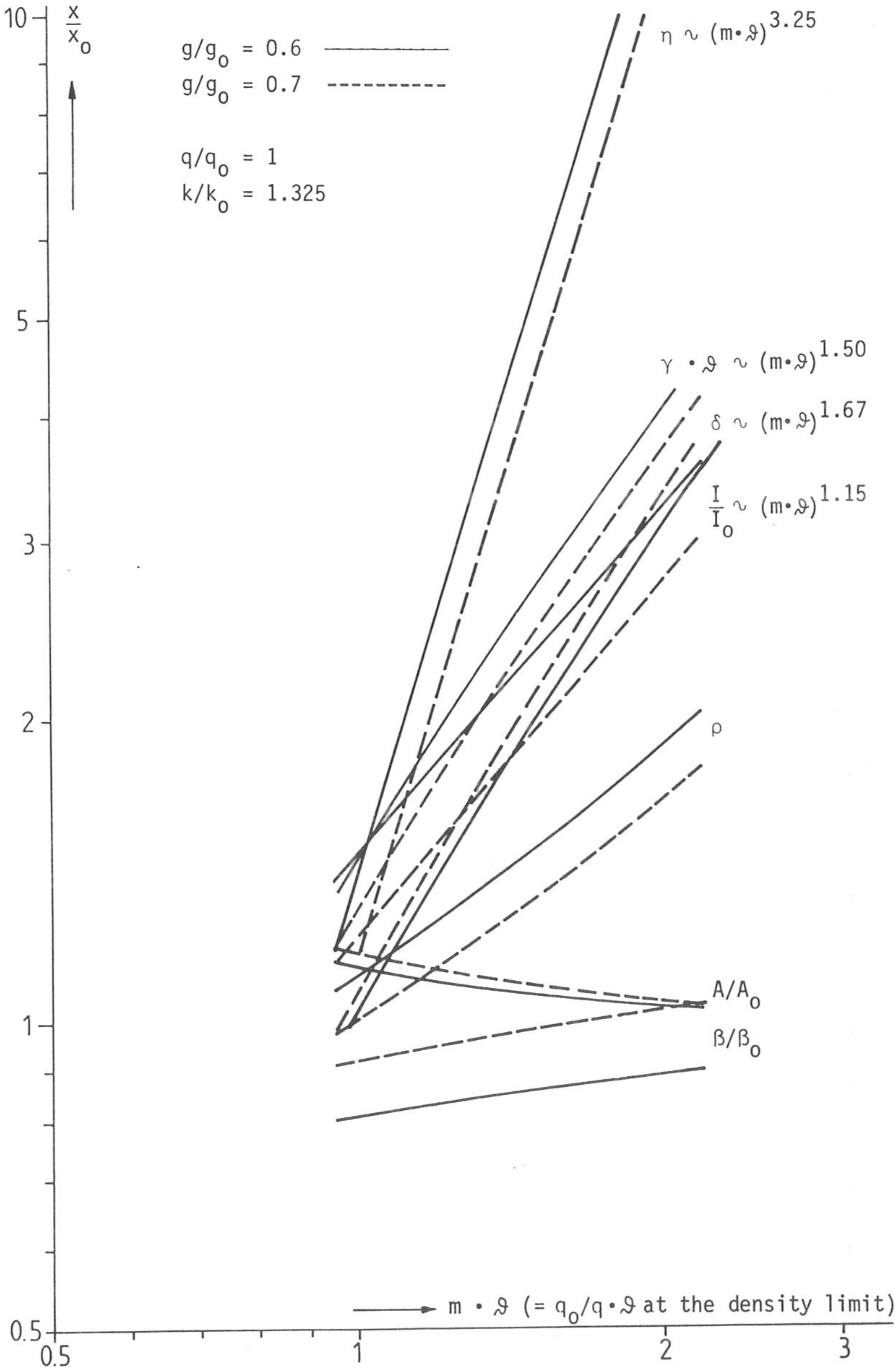

Fig. 13: Reactor rescaling based on the INTOR configuration for fixed q/q_o and k/k_o

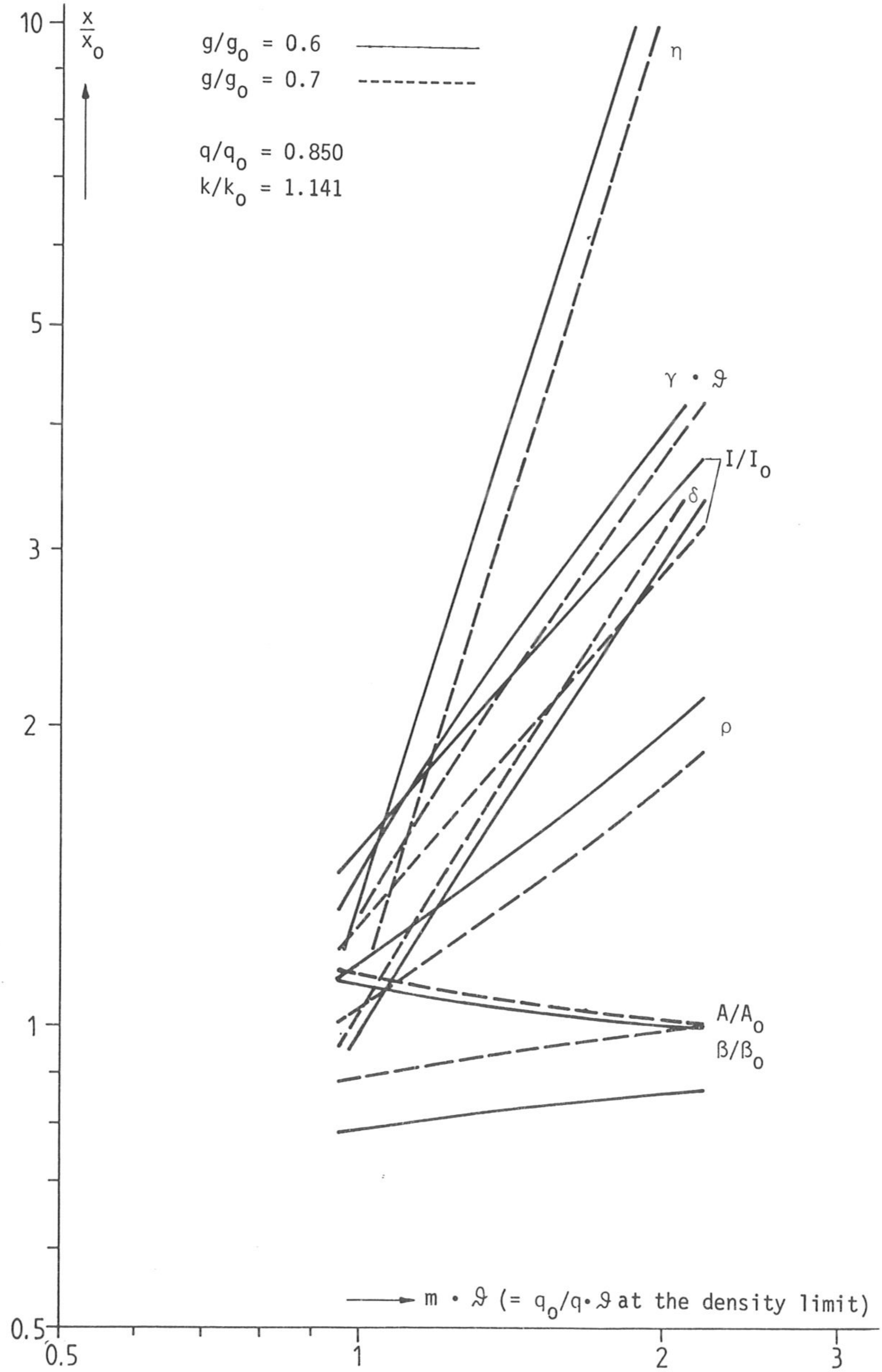

Fig. 14: Reactor rescaling based on the INTOR configuration fixed for q/q_o and k/k_o

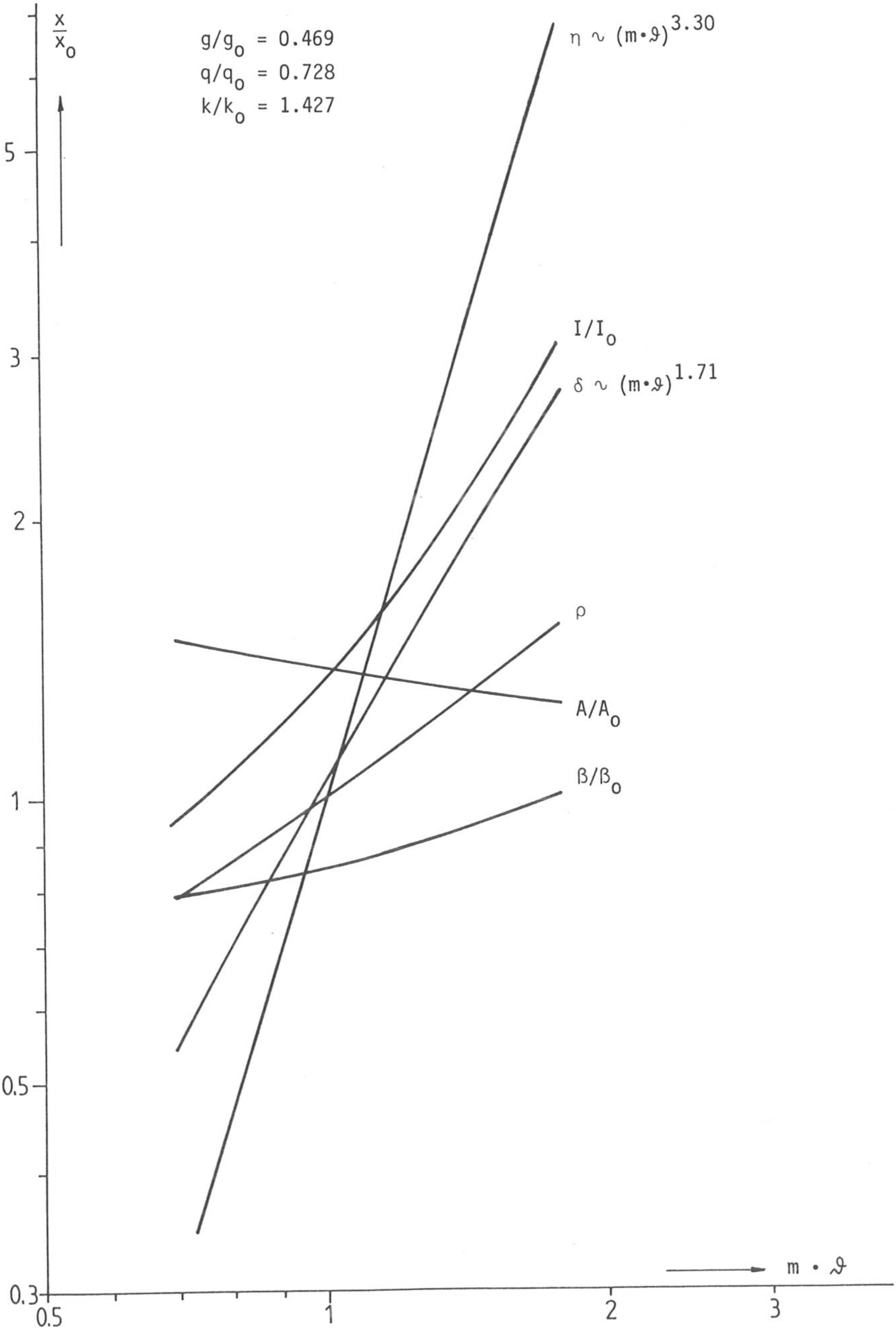

Fig. 15: Reactor rescaling based on the STARFIRE configuration

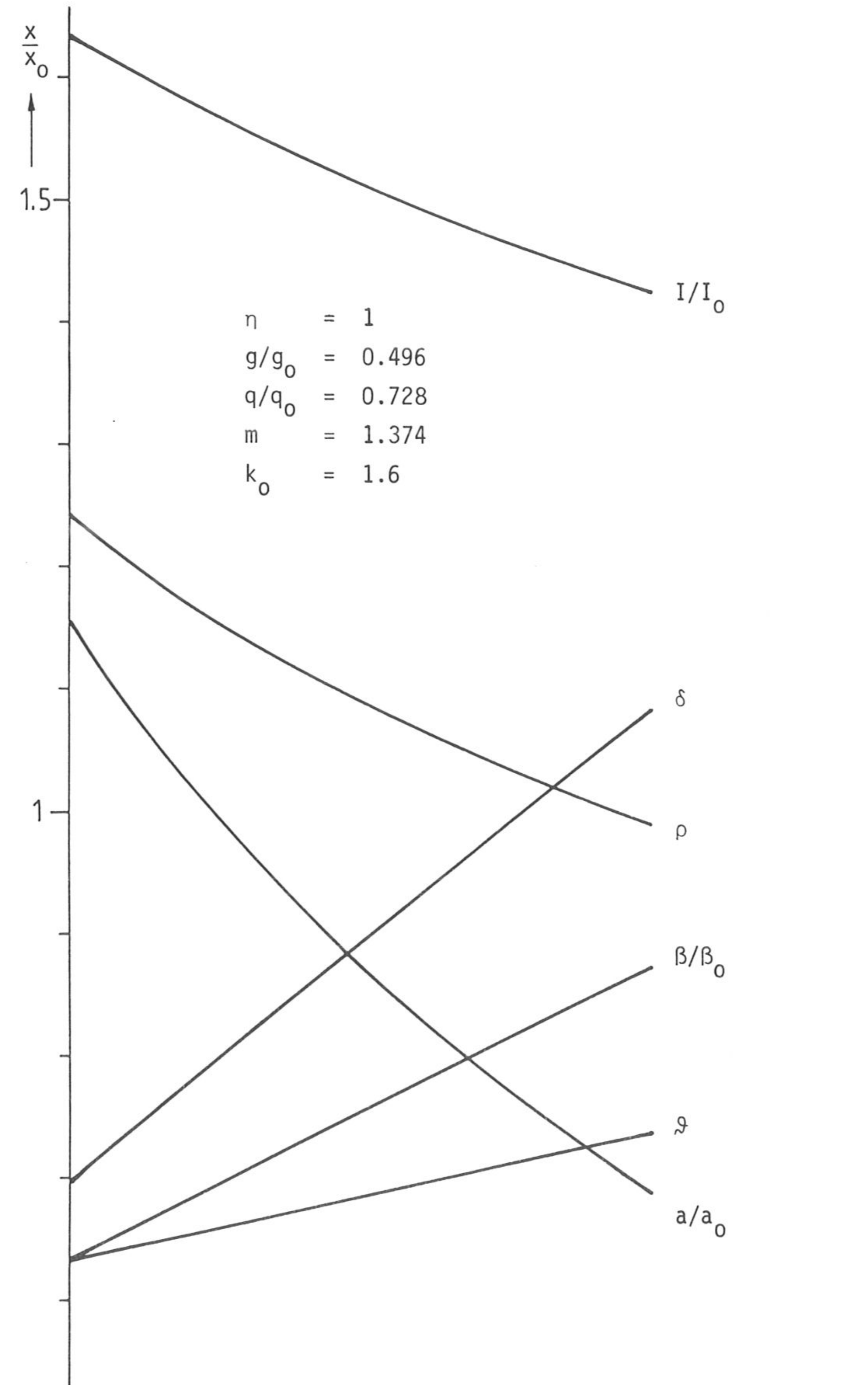

Fig. 16: STARFIRE alternatives

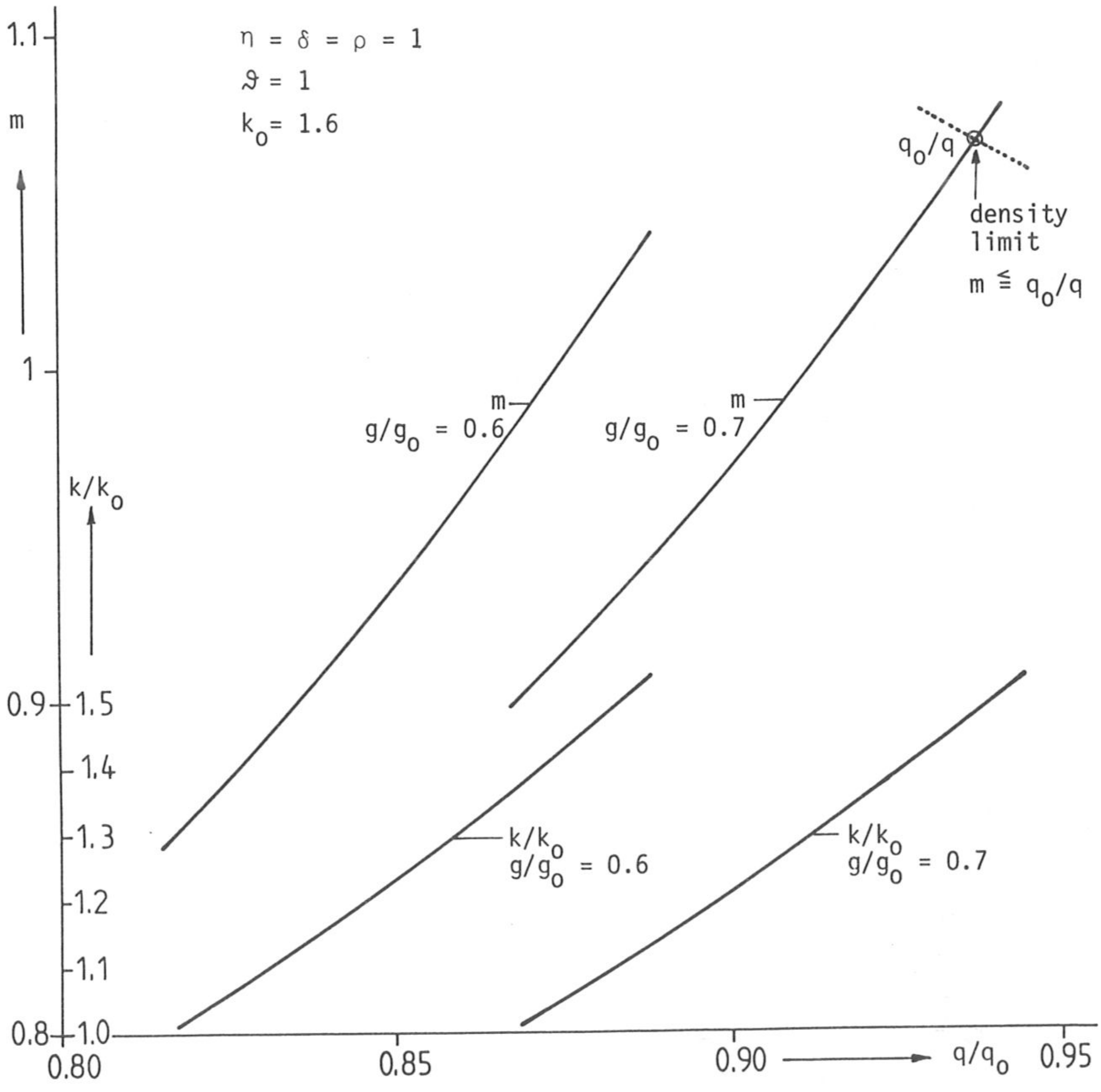

Fig. A1: INTOR rescaling for $\eta = \delta = \rho = 1$ - elongation and Murakami-parameter vs. reduced safety factor.

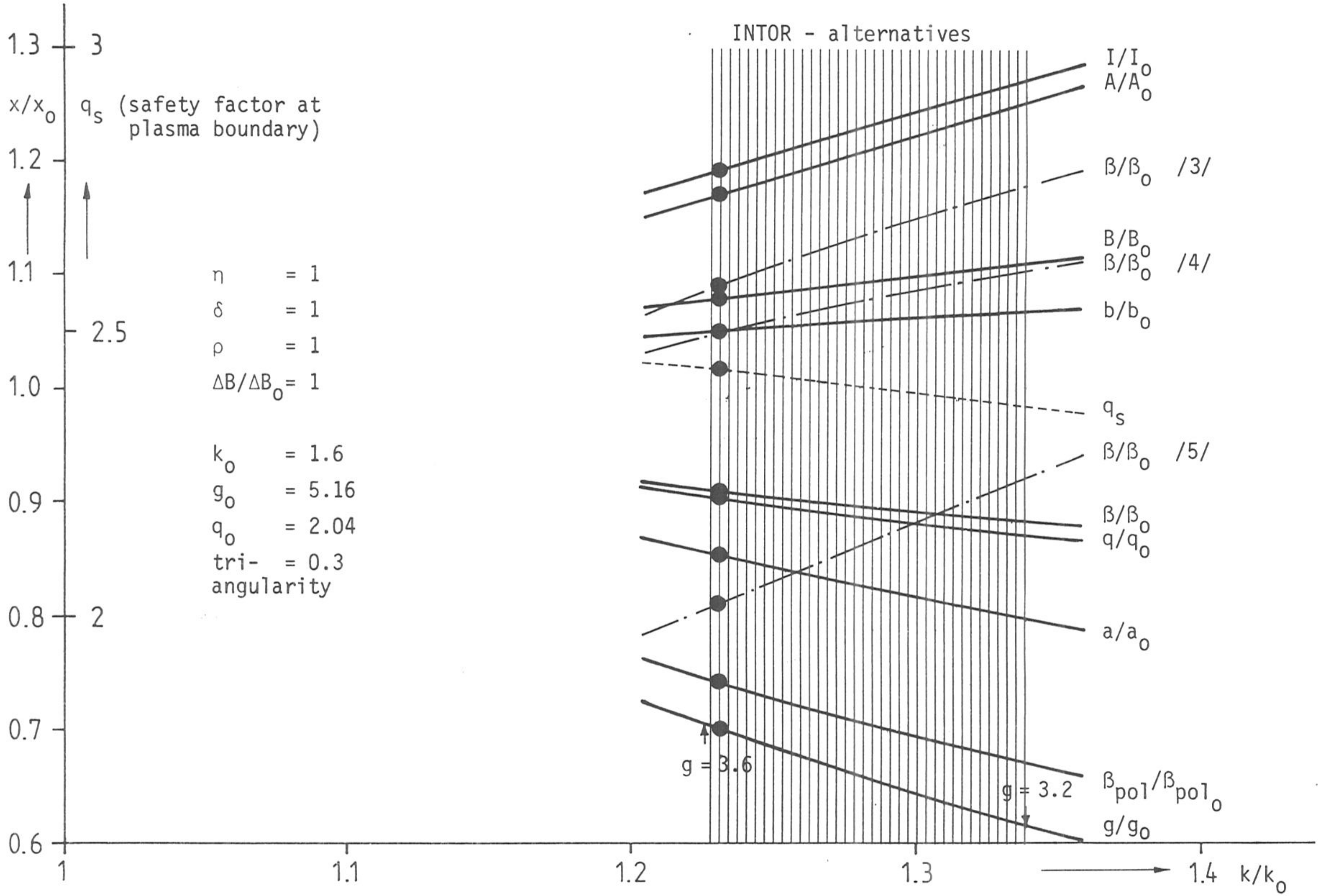

Fig. A2: INTOR rescaling for $\eta = \delta = \rho = 1$ (reduced alpha and impurity contribution to β_o)